Supplementary Material

Coreactant-free polyfluorene nanoparticles for the electrochemiluminescence quantitative analysis of dopamine and norepinephrine

Guomin Yang, Kejun Tan*, Jun Yang, Ruo Yuan, Shihong Chen*

Key Laboratory of Luminescence Analysis and Molecular Sensing (Southwest University), Ministry of Education, College of Chemistry and Chemical Engineering, Southwest University, Chongqing 400715, PR China

Table of contents

*Corresponding author **Tel:** +86-23-68253172 **Fax:** +86-23-68253172
E-mail address: tankj@swu.edu.cn (K. Tan); cshong@swu.edu.cn (S. Chen)

Materials

Poly[(9,9-dioctylfluorenyl-2,7-diyl)-*co*-(1,4-benzo-{2,1',3}-thiadazole)] (PFBT, MW~134000, polydispersity 3.5) was purchased from ADS Dyes Source, Inc (Quebec, Canada). Poly(styrene-*co*-maleicanhydride) (PSMA, MW~1700, styrene content 68%), dopamine hydrochloride (98%) and uric acid (99%) were provided by Aladdin Ltd. (Shanghai, China). L-Epinephrine hydrochloride (98%), L-cysteine and histidine were bought from Shanghai Macklin Biochemical Co., Ltd. (Shanghai, China). Chengdu Kelon Chemical Co., Ltd. (Chengdu, China) provided glucose (monohydrate), glycine, L-arginine and ascorbic acid. Tixi Ai Chemical Industrial Development Co., Ltd. (Shanghai, China) provided tetrahydrofuran (THF, anhydrous, ≥99.9%). Phosphate buffer solution (PBS) was prepared by using 0.10 M Na_2HPO_4, 0.10 M KH_2PO_4 and 0.10 M KCl. Artificial cerebral spinal fluid (ACSF) was made up of NaCl (150 mM), KCl (3.0 mM), $CaCl_2 \cdot 2H_2O$ (1.4 mM), $MgCl_2 \cdot 6H_2O$ (0.8 mM) and phosphate (1.0 mM). The above reagents are all analytically pure, and ultrapure water was used throughout the experiment.

Instruments

MPI-E electrochemiluminescent analysis system (Xi'an Remax Analyse Instrument Co. Ltd, Xi'an, China) was used to collect ECL signals. Cyclic voltammetry (CV) and electrochemical impedance spectroscopy (EIS) measurements were carried out by CHI660D electrochemical work station (Shanghai CH Instruments, Shanghai, China) in 5.0 mM $K_3[Fe(CN)_6]/K_4[Fe(CN)_6]$ (1:1). JEM 1200EX microscope (JEOL Co. Ltd, Janpan) was used to collect transmission electron microscopy (TEM) images. A

Escalab 250Xi spectrometer (Thermo Scientific, USA) and a Nicolet 6700 Fourier transform infrared (FI-IR) spectrometer (FEI, USA) were respectively used to record X-ray photoelectron spectroscopy (XPS) and FT-IR spectra. Ultraviolet-visible (UV-vis) spectra were collected on a Lambda 17 UV-vis spectrometer (PE Co. Ltd, USA). Contact angle and zeta potential were measured on DSA25 contact angle goniometer (KRUSS, Germany) and Malvin nanometer potentiometer (Malvern, UK), respectively. The ECL emission spectrum was obtained from a CHI 760E combined with a Newton EMCCD spectroscopy detector (Andor, Tokyo, Japan).

Water contact angles, zeta potential detection and XRD pattern

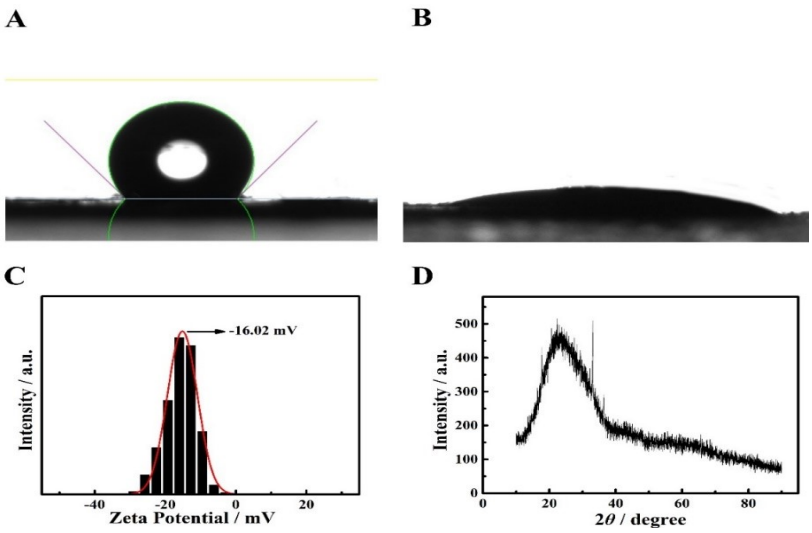

Fig. S1 Water contact angles of (A) PFBT and (B) PFBT NPs; (C) Zeta potential and (D) XRD pattern of PFBT NPs.

Comparison of ECL intensity of PFBT and PFBT NPs

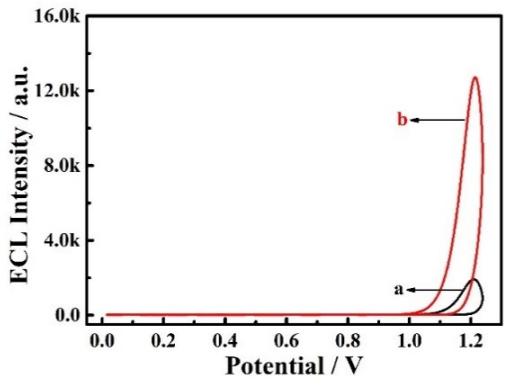

Fig. S2 ECL responses of (a) PFBT/GCE and (b) PFBT NPs/GCE in PBS (0.10 M, pH 7.4). Potential scanning range of 0 ~ +1.25 V, scan rate of 0.30 V/s, amplifier series of 4 and PMT potential of 700 V.

Experimental details of the ECL spectrum measurements

The ECL spectrum of PFBT NPs was collected on a CHI 760E combined with a Newton EMCCD spectroscopy detector. First of all, 12 μL of PFBT NPs dispersion was dripped onto the clean GCE (Φ = 4 mm) surface and dried in air overnight to obtain PFBT NPs modified GCE (PFBT NPs/GCE). Then, the ECL emission spectrum was collected in 0.10 M PBS (3.0 mL, pH 7.4) using a three-electrode system consisting of counter electrode (platinum wire electrode), reference electrode (Ag/AgCl (saturated KCl) electrode) and working electrode (modified glassy carbon electrode). The potential scanning range of 0 ~ +1.25 V was adopted.

ECL quenching mechanisms

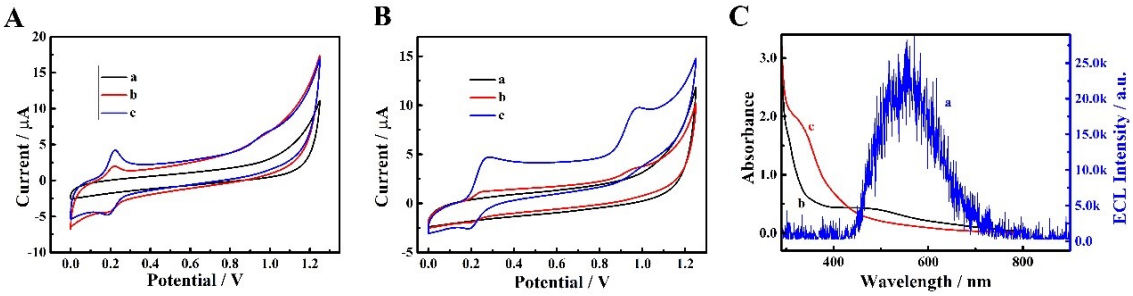

Fig. S3 (A) CV profiles of bare GCE (a) without, (b) with 1.0×10^{-5} M and (c) with 3.0×10^{-5} M DA in 0.10 M PBS (pH 7.4); (B) CV curves of bare GCE (a) without, (b) with 1.0×10^{-4} M and (c) with 2.0×10^{-4} M NE in 0.10 M PBS (pH 7.4). Scan potential: 0 ~ +1.25 V. Scanning rate: 100 $mV\cdot s^{-1}$. (C) (a) ECL spectrum of PFBT NPs; UV-vis absorption spectra of (b) oxidized DA and (c) oxidized NE.

Optimization of experimental conditions

To ensure that the sensor possessed the best performance, the modification amount of the PFBT NPs dispersion (0.05 mg/mL) on the electrode (GCE) was optimized and corresponding ECL response was detected in 3.0 mL of PBS (0.10 M, pH 7.4). As

depictured in Fig. S4A, the ECL signal of PFBT NPs/GCE gradually increased with the modification amount increasing from 6.0 μL to 12 μL. When the modification amount surpassed 12 μL, the ECL intensity has exceeded the detection range. Hence, in order to ensure the accuracy of the experiment, 12 μL was selected as the optimal modification amount. Subsequently, the ECL signals of the GCE modified with 12 μL PFBT NPs dispersion were examined in 0.10 M PBS at different pH (Fig. S4B). As the pH increased from 4.0 to 10, the ECL intensity of the PFBT NPs/GCE rose. Then, the ECL response value of PFBT NPs/GCE was beyond the detection range of the instrument after pH exceeding 10 (the data not shown here). Moreover, considering that the ECL signal at pH 7.4 was strong enough to meet the sensitivity requirement of DA and NE detection and the physiological pH was also 7.4, pH 7.4 was chosen as the optimal pH for DA and NE detection.

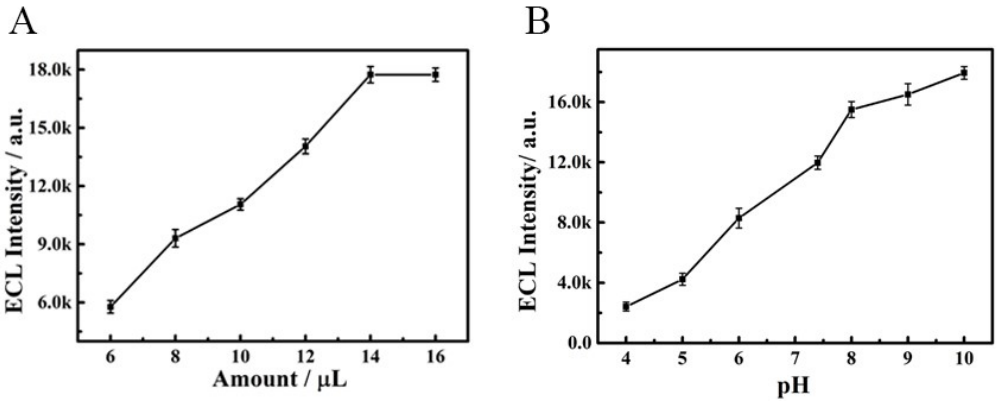

Fig. S4 Effect of (A) modification amount of PFBT NPs and (B) pH of PBS (0.10 M) on ECL response of sensor. Potential scanning range of 0 ~ +1.25 V, scan rate of 0.30 V/s, amplifier series of 4 and PMT potential of 700 V for ECL.

Comparison of the constructed sensor with previously reported strategies

Table S1. Comparison the analytical results of different strategies for DA and NE detection

Method	target	linear range (M)	LOD (M)	References
ECL	DA	1.0×10^{-9}–1.0×10^{-6}	8.5×10^{-10}	1
Fluorescence	DA	1.0×10^{-7}–2.0×10^{-5}	4.0×10^{-8}	2

Fluorescence	DA	1.0×10^{-7}–1.0×10^{-5}	6.8×10^{-8}	3
DPV	DA	5.0×10^{-7}–5.0×10^{-5}	2.0×10^{-8}	4
Colorimetry	DA	0–6.0×10^{-7}	6.0×10^{-5}	5
DPV	NE	1.0×10^{-7}–5.6×10^{-4}	6.0×10^{-8}	6
DPV	NE	5.0×10^{-7}–3.2×10^{-5}	6.0×10^{-9}	7
FI–ECL	NE	4.0×10^{-8}–1.0×10^{-5}	2.5×10^{-8}	8
UPLC-MS/MS	NE	3.0×10^{-7}–1.5×10^{-4}	1.5×10^{-10}	9
ECL	NE	8.0×10^{-9}–8.0×10^{-7}	8.2×10^{-10}	10
ECL	DA	1.0×10^{-9} –1.0×10^{-4}	4.0×10^{-10}	This work
ECL	NE	5.0×10^{-9}–5.0×10^{-4}	1.2×10^{-9}	This work

Selectivity of the sensor

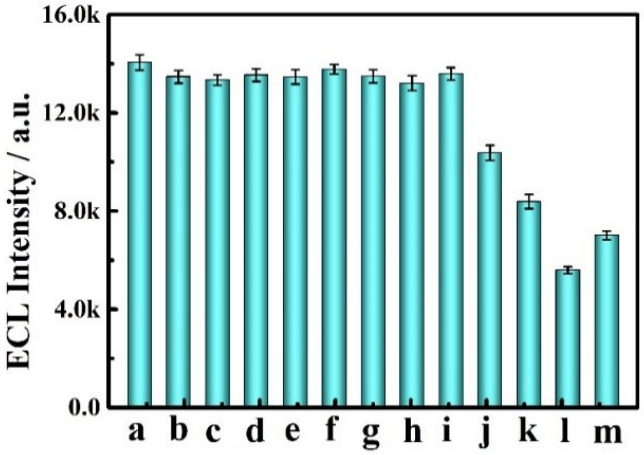

Fig. S5 ECL response of sensor toward different substances: from a to m: blank, AA, UA, Glu, K+, Gly L-Arg, L-Cys, His, 5-HT, Ep, DA and NE.

Storage stability of the sensor

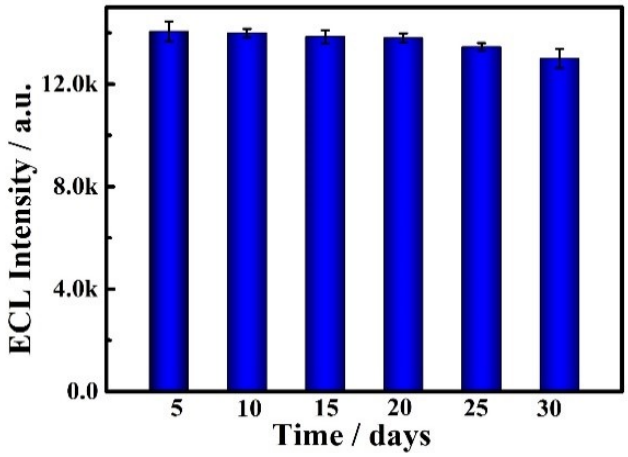

Fig. S6 Storage stability of PFBT NPs/GCE. Test conditions: the test solution (0.10 M PBS, 3.0 mL, pH 7.4), potential scanning range (0 ~ +1.25 V), scan rate (0.3 V/s), amplifier series (4) and potential of photomultiplier tube (700 V)

Recovery tests of DA and NE in ACSF

Table S2 Recovery results of DA in ACSF samples by HPLC and ECL in this work.

Sample	c_{add}/μM	[a]$c_{detected}$/μM±[b]SD (HPLC)	Recovery %(HPLC)	[a]$c_{detected}$/μM±[b]SD (ECL)	Recovery %(ECL)	*E*r %
1	100	101±3	101	103±3	103	2.0
2	50.0	48.2±1.7	96.4	47.4±2.1	94.8	-1.7
3	5.00	4.95±0.23	99.0	5.21±0.22	104	5.3

[a]Average of three determinations; [b]standard deviation (SD) of three measurements.

Table S3 Recovery results of NE in ACSF samples by HPLC and ECL in this work.

Sample	c_{add}/μM	[a]$c_{detected}$/μM±[b]SD (HPLC)	Recovery %(HPLC)	[a]$c_{detected}$/μM±[b]SD (ECL)	Recovery %(ECL)	*E*r %
1	100	105±4	105	106±3	106	1.0
2	50.0	48.9±0.5	97.8	50.2±0.7	100	2.7
3	5.00	5.12±0.13	102	5.23±0.22	105	2.2

[a]Average of three determinations; [b]standard deviation (SD) of three measurements.

Calculation of detection limit and quantification limit

The detection limit (LOD) was calculated according to the traditional approach reported in previous literature.[11] First, an ECL measurement for blank samples was carried out with three parallel tests, which showed an average ECL intensity (I_B) and a standard deviation (S_B). Then, the smallest detectable signal (I_L) was calculated according to equation (1), in which the numerical factor k was chosen as 3 at a desired confidence level of 99.86%.

$$I_L = I_B + k \times S_B \quad (1)$$

In this work, three parallel tests for a blank sample showed that I_B and S_B were calculated as 14052.5 and 73.1, respectively. The I_L was calculated as 14271.91 through equation (1).

For DA analysis, the linear regression equation was expressed as I = -1959.13 lg c_1 - 4086.58, thus the c_1 can be calculated as 4.0×10^{-10} M when $I = I_L$ = 14271.91,

representing the LOD. Then, the LOD of NE analysis was obtained in the similar calculation method. The linear regression equation of was fitted as I = -1801.30 lg c_2 - 1794.22. Thus, the LOD was calculated as 1.2×10^{-9} M.

The limit of quantification (LOQ) was calculated referring to previous literature.[12] Initially, the blank sample was performed ECL measurement with three parallel tests to obtain ECL intensity values (I_B). Subsequently, the obtained three ECL intensity values were respectively put into the linear regression equation of DA or NE analysis to obtain three corresponding concentration values (c), thus the mean concentration (X_{b1}) and standard deviation (S_{b1}) of the blank were calculated. Then, the LOQ was calculated according to equation (2).

$$LOQ=X_{b1}+10S_{b1} \qquad (2)$$

In our work, three parallel tests for a blank sample displayed that I_B were 13954.1, 14129.3 and 14074.1, respectively. For DA analysis, the linear regression equation was expressed as I = -1959.13 lg c_1 - 4086.58, thus $X_{b1} = 5.5\times10^{-10}$ M and $S_{b1} = 5.9\times10^{-11}$ M were calculated when $I = I_B$. Therefore, the LOQ of DA analysis was calculated as 1.1×10^{-9} M through equation (2).

The LOQ of NE analysis was obtained in the similar calculation method. According to the linear regression equation of NE detection of I = -1801.30 lg c_2 - 1794.22, X_{b1} and S_{b1} were severally calculated as 1.6×10^{-9} M and 1.9×10^{-10} when $I = I_B$. Hence, LOQ of NE analysis was calculated as 3.5×10^{-9} M according to equation (2).

References

1 L. Cui, S. L. Yu, W. Q. Gao, X. M. Zhang, S. Y. Deng and C. Y. Zhang, *ACS Appl.*

Mater. Interfaces., 2020, **12**, 7966−7973.

2 A. Yildirim and M. Bayindir, *Anal. Chem.*, 2014, **86**, 5508−5512.

3 K. Qu, J. Wang, J. Ren and X. Qu, *Chemistry*, 2013, **19**, 7243–7249.

4 M. Liu, Q. Chen, C. Lai, Y. Zhang, J. Deng, H. Li and S. Yao, *Biosens. Bioelectron*., 2013, **48**, 75–81.

5 Y. Lin, C. Chen, C. Wang, F. Pu, J. Ren and X. Qu, *Chem. Commun*., 2011, **47**, 1181–1183.

6 M. Taei and M. S. Jamshidi, *Microchem. J.*, 2017, **130**, 108–115.

7 M. Y. Emran, M. Mekawy, N. Akhtar, M. A. Shenashen, I. M. EL-Sewify, A. Faheem and S. A. El-Safty, *Biosens. Bioelectron.*, 2018, **100**, 122–131.

8 F. Li, Y. Q. Pang, X. Q. Lin and H. Cui, *Talanta*., 2003, **59**, 627–636.

9 C. Ji, J. Walton, Y. Su and M. Tella, *Anal. Chim. Acta*., 2010, **670**, 84–91.

10 X. Y. Chen, R. J. Zheng, L. Q. Ren and J. J. Sun, *RSC Adv.*, 2016, **6**, 16495–16499.

11 G. L. Long and J. D. Winefordner, *Anal. Chem*., 1983, **55**, 712–724.

12 A. Shrivastava and V. B. Gupta, *Chron. Young Sci,* 2011, **2**, 21-25.